Engl. **28**, 1283 (1989); *Acc. Chem. Res.* **22**, 287 (1989).
4. D. K. Lavallee, *Mol. Struct. Energ.* **9**, 279 (1988).
5. H. A. Dailey and J. E. Fleming, *J. Biol. Chem.* **258**, 11,453 (1983).
6. D. K. Lavallee, *The Chemistry and Biochemistry of N-Substituted Porphyrins* (VCH, New York, 1988).
7. F. R. Hopf and D. G. Whitten, in *The Porphyrins*, D. Dolphin, Ed. (Academic Press, New York, 1978), vol. 2, pp. 161–195.
8. W. I. White, *ibid.*, vol. 5, pp. 303–339.
9. F. Li, C. K. Lim, T. J. Peters, *Biomed. Chromatogr* **2**, 164 (1987).
10. R. G. Roberts, *ibid.*, **2**, 71 (1987).
11. E. Rossi, K. A. Costin, P. Garcia-Webb, *Clin. Chem.* **34**, 2481 (1988).
12. Carrier proteins bovine serum albumin and ovalbumin were treated with the *bis-N*-hydroxysuccinimide ester of hapten **1**. Epitope densities ranged from five to ten haptens per carrier monomer. Swiss-Webster mice were immunized, and spleen cells were fused with the myeloma line SP 2/0. Binding of these antibodies to hapten-protein conjugates was completely inhibited by preincubation of cell culture supernatants with 50 μg/ml (86 μM) free hapten. Antibodies [immunoglobulin G1 (IgG1)] were purified from ascites fluid by Protein A affinity chromatography and were determined to be >95% IgG by denaturing polyacrylamide gel electrophoresis [U. Laemmli, *Nature* **227**, 680 (1970)]. Protein concentrations were determined by Bradford assay [M. M. Bradford, *Anal. Biochem.* **72**, 248 (1976)] and by absorbance at 280 nm.
13. Reactions were assayed (*9*) by reversed-phase high-performance liquid chromatography with a Hewlett-Packard Model 1190L Liquid Chromatograph equipped with a Waters Associates Model 625 Diode-Array Detector, a Hewlett-Packard Model 3396A Integrator, and a Dynamax C18 column (4.6 mm by 25 cm, 5-μm particle size, Rainin Instruments). Mobil phase consisted of 0 to 15% 1 M ammonium acetate, pH 5.2, in methanol. Various isocratic or gradient elutions were performed depending on the retention characteristics of the particular porphyrins in the mixture. Detection was at 390 nm for Cu(II) mesoporphyrin, 370 nm for Mn(III) mesoporphyrin, 410 nm for Co(III) mesoporphyrin, 420 nm for Co(III) protoporphyrin, and 400 nm for all other porphyrins. Reaction aliquots (40 μl) were mixed with 160 μl of 30% dimethylsulfoxide (DMSO) (v/v) in methanol containing 1 to 5 μM of an appropriate metalloporphyrin as an internal standard. After filtration, this mixture was directly injected onto the column. Plots of product: internal standard area ratios versus product concentration were linear for solutions containing up to 40 μM product. Reaction mixtures (300 μl) contained porphyrin, metal salt, 90 mM tris acetate, pH 8.0, 0.5% (w/v) Triton X-100, and 5% (v/v) DMSO. Antibody reactions additionally contained 50 μg of protein per milliliter (0.3 μM). Reactions were incubated at 26°C.
14. I. H. Segel, *Enzyme Kinetics* (Wiley-Interscience, New York, 1975), pp. 59–61.
15. A. W. Schwabacher, M. I. Weinhouse, M.-T. M. Auditor, R. A. Lerner, *J. Am. Chem. Soc.* **111**, 2344 (1989).
16. Deuteroporphyrin metallation was assayed with Zn^{2+}. Protoporphyrin metallation was assayed with Cu^{2+} and Co^{2+}.
17. S. Taketani and R. Tokunaga, *J. Biol. Chem.* **256**, 12,748 (1981).
18. ———, *Eur. J. Biochem.* **127**, 443 (1982).
19. The ultraviolet-visible spectrum of mesoporphyrin (10 μM) in reaction buffer was compared to the spectrum in the presence of excess antibody. A slight red-shift of 1 to 2 nm (397 to 398 nm, Soret band) was detected upon binding to antibody. No change was observed in the relative positions or intensities of the visible bands. In particular, the spectrum bore no similarity to that of the hapten.
20. R. F. Pasternack, N. Sutin, D. H. Turner, *J. Am. Chem. Soc.* **98**, 1908 (1976).
21. We thank P. R. Ortiz de Montellano for helpful discussions and R. Ranon for production of antibodies. Financial support was provided by Affymax Research Institute, the Office of Naval Research (ONR N0014-87-K-0256), an NSF Waterman Award (CHE-8451306) to P.G.S., and by Schering-Plough to A.G.C.

2 May 1990; accepted 28 June 1990

External Guide Sequences for an RNA Enzyme

ANTHONY C. FORSTER AND SIDNEY ALTMAN*

Ribonuclease P (RNase P) from *Escherichia coli* or its catalytic RNA subunit can efficiently cleave small RNA substrates that lack the conserved features of natural substrates of RNase P if an additional small RNA is also present. This additional RNA must contain a sequence complementary to the substrate [external guide sequence (EGS)] and a 3′-proximal CCA sequence to ensure cleavage. The aminoacyl acceptor stem and some additional 5′- and 3′-terminal sequences of a precursor transfer RNA are sufficient to allow efficient cleavage by RNase P, and the 2′-hydroxyl group at the cleavage site is not absolutely necessary for cleavage. In principle, any RNA could be targeted by a custom-designed EGS RNA for specific cleavage by RNase P in vitro or in vivo.

ALL REACTIONS THAT ARE GOVerned by RNA in vivo result in the transesterification or hydrolysis of specific phosphodiester bonds in RNA. In several classes of these reactions, an intramolecular site of cleavage or ligation is identified by internal guide sequences (IGSs) which form base pairs with the segment of the phosphodiester chain that contains the cleavage site (*1*). However, IGSs are not present in the class of reactions governed by RNA that are enzymatic in vivo, namely, the cleavage of precursor tRNA molecules by the RNA component of eubacterial RNase P (*2, 3*). The nucleotide sequence of the segment of the phosphodiester chain that contains the cleavage site is not conserved among different substrates for RNase P (*4*), so it cannot be recognized by a unique IGS in the enzyme. We propose that the 3′-proximal sequence of the acceptor stem of a precursor tRNA can be regarded as an "external guide sequence" (EGS; Fig. 1A) because it identifies the site of cleavage, in part, by forming base pairs with the segment of the phosphodiester chain that is cleaved. In contrast to IGSs, which are covalently attached to a "catalytic" sequence in vivo, EGSs are external to the native enzyme and are highly variable. We show that an EGS is essential for cleavage of a substrate by RNase P from *E. coli* and that the EGS is still functional when detached from the substrate. We have used EGS-containing RNAs (EGS RNAs) to construct a very small model substrate for RNase P and to investigate the mechanism of recognition and cleavage of the substrate. Furthermore, we propose that any RNA may be targeted for specific cleavage in vitro or in vivo by RNase P provided that the RNA is associated with a custom-designed EGS RNA.

The importance of the EGS for cleavage by RNase P was tested with derivatives of the smallest model substrate reported to be cleaved efficiently by RNase P, pAT1 [Fig. 1B; (*5*)]. As anticipated from previous work (*5*), derivatives of pAT1 with 3′-terminal truncations that deleted the EGS, termed Hinf I pAT1 and Taq I pAT1 [these RNAs consist of the 5′-terminal 24 and 31 nucleotides (nt) of pAT1, respectively; Fig. 1B], were not cleaved by RNase P from *E. coli* (M1 RNA plus C5 protein) or by M1 RNA under conditions where pAT1 was cleaved efficiently (Fig. 2, lanes 1 through 4; pAT1, Hinf I pAT1, and Taq I pAT1 are represented by P, H, and T, respectively). However, if an RNA that contained the deleted EGS [either the 29-nt EGS RNA or the 20-nt EGS RNA (Fig. 1, C and D)] was added to the reaction mixture, Hinf I pAT1 and Taq I pAT1 were cleaved efficiently at the same cleavage site as in pAT1 (Fig. 2, lanes 6, 7, 9, and 10). The 20- and 29-nt EGS RNAs did not stimulate the cleavage of pAT1 by M1 RNA or RNase P (Fig. 2, lanes 2, 5, and 8). In addition, a 17-nt RNA, designed such that a substrate and an EGS RNA could be made from the same sequence (Fig. 1E), was also cleaved efficiently by RNase P (Fig. 2B, lanes 11 and 12), but was cleaved poorly by M1 RNA (Fig. 2A, lanes 11 and 12). Although the 17-nt RNA contains the same octanucleotide 3′-terminal sequence as the 20- or 29-nt EGS RNAs, Hinf I pAT1 and Taq I pAT1 were not cleaved by M1 RNA or by RNase P in the presence of the 17-nt RNA, indicating that the functions of the 20- and 29-nt EGS RNAs were not just

Department of Biology, Yale University, New Haven, CT 06520.

*To whom correspondence should be addressed.

due to their eight 3′-terminal nucleotides. Nevertheless, at least one of the three 3′-terminal nucleotides of pAT1 (and presumably the 20- and 29-nt EGS RNAs) is important because derivatives of pAT1 with small 3′-terminal truncations, termed Ban I pAT1, N1a IV pAT1, and Bsp 1286 pAT1 (Fig. 1B), did not function as substrates under precisely the same conditions as in Fig. 2, lanes 2. This result is not surprising because base substitutions for the 5′-proximal C of the $CCAC_{OH}$ sequence of pAT1 drastically reduce cleavage (*5*). Therefore, in our system at least part of both the EGS and the conserved CCA sequence are necessary for efficient cleavage.

The results with Hinf I pAT1–20-nt EGS RNA and Taq I pAT1–20-nt EGS RNA demonstrate that EGSs longer than the 7-nt EGS present in the aminoacyl acceptor stem of precursor tRNAs (Fig. 1A) are functional and that the conserved GUUC loop of precursor tRNAs is unnecessary for efficient cleavage by RNase P. The result with the 17-nt RNA demonstrates that a small portion of a precursor tRNA is sufficient for efficient cleavage by RNase P: the aminoacyl acceptor stem and some additional 5′- and 3′-terminal sequences. The site of cleavage of the 17-nt RNA [Fig. 1E (*6, 7*)] is in a potentially double-stranded region, as is the case for many substrates of RNase P found in vivo (*4*). The poor cleavage of the 17-nt RNA by M1 RNA (not RNase P) may have been caused by the base-pairing of the nucleotide on the 5′ side of the cleavage site. It seems that the location of the site cleaved by M1 RNA and RNase P was determined by the position of the conserved CCA sequence, not the junction of the single- and double-stranded regions. This may prove to be a general rule for the selection of the cleavage site in all substrate–EGS RNA complexes, but it is known that some other RNase P substrates are either cleaved one nucleotide away from the expected cleavage site (*8*) or are cleaved accurately in the absence of the CCA sequence (*9*).

RNase P generates cleavage products with 5′ phosphate and 3′-OH termini in a hydrolysis reaction that leaves the adjacent 2′-OH group unchanged (*3*). In the case of RNase P from the nucleus of the yeast *Saccharomyces cerevisiae* (*10*), this 2′-OH is unnecessary for cleavage because a molecule consisting of a short oligodeoxyribonucleotide attached to the 5′ end of a tRNA can be cleaved specifically at the junction between the DNA and the RNA (*11*). Since eukaryotic RNase P ribonucleoproteins contain RNA components that have not yet been shown to have catalytic activity in vitro (*3, 10*), it is important to ascertain whether mechanistic similarities exist between the two classes of RNase P. An analog of the 17-nt RNA (Fig. 1E) containing a 2′-H only at the cleavage site (termed 17-nt:dT) was prepared by transcription in the presence of [α-^{32}P]deoxythymidine 5′-triphosphate (dTTP) instead of uridine 5′-triphosphate (UTP) (*12*). Despite a greatly reduced yield of the full-length transcript, a sufficient amount of 17-nt:dT was obtained to determine that, in the presence of excess RNase P, cleavage occurred at the same site as in the 17-nt RNA, but with a 45-fold decrease in the velocity (*13*). Hence, the mechanism of cleavage by a eubacterial RNase P, as is the case with a eukaryotic RNase P (*11*) and a self-splicing group I intron (*14*), is not absolutely dependent on the presence of a 2′-OH at the cleavage site. This supports proposals that suggest that the 2′-OH at the cleavage site does not directly participate in the RNase P cleavage reaction (*15*). However, the lower rate of cleavage of 17-nt:dT in comparison to that of the 17-nt RNA suggests that the 2′-OH may play an indirect role in the reaction mechanism. For example, it may stabilize an adjacent 3′-O^- leaving group through a combined electron-withdrawing effect and hydrogen bonding (*16*), or it may bind to water, Mg^{2+}, or RNA groups at the active center of the enzyme. Replacement of either Hinf I pAT1 or the 29-nt EGS RNA by a synthetic oligodeoxyribonucleotide of identical sequence in reactions of M1 RNA or RNase P with Hinf I pAT1–29-nt EGS RNA abol-

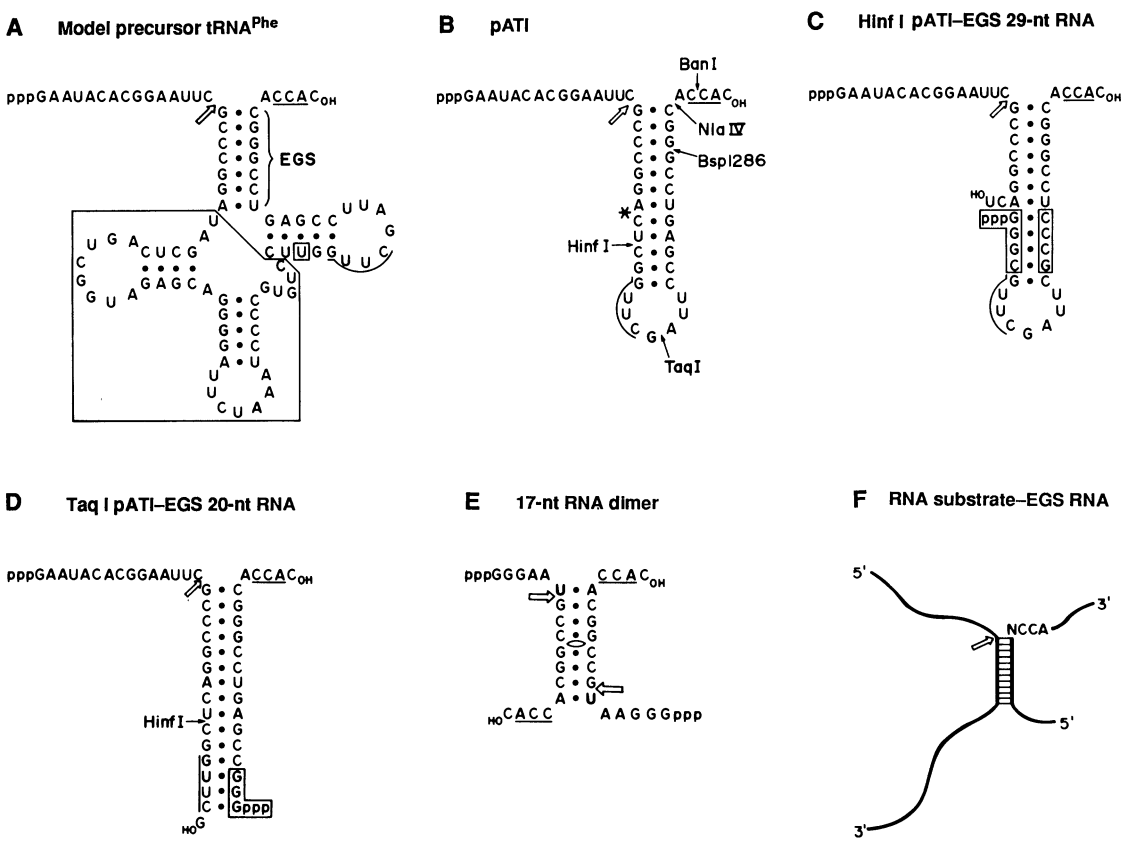

Fig. 1. Sequences and proposed secondary structures of substrates [**A** and **B**; (*5*)] and complexes between substrates and EGS RNAs (**C** through **F**). Open arrows mark the sites of cleavage by M1 RNA and RNase P. Thin arrows mark the 3′ termini of truncated derivatives of pAT1 synthesized from the plasmid template for pAT1 after digestion with the indicated restriction endonuclease. Sequences of three or more nucleotides that are invariant in all precursor tRNAs from *E. coli* (*4*) are underlined. Nucleotides in (A), (C), and (D) that differ from those in (B) are boxed. The asterisk in (B) identifies the phosphodiester bond that is not present in (A). The symmetry element present in the double-helical structure of (E) is a C_2 proper axis of rotation.

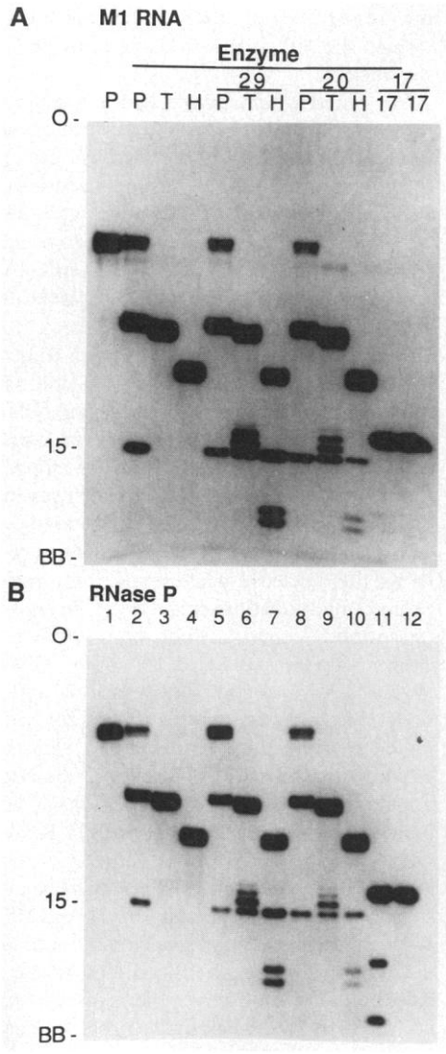

Fig. 2. Assay of substrates for cleavage by (**A**) M1 RNA or (**B**) RNase P in the presence or absence of EGS RNAs. A mixture of unlabeled and [α-^{32}P]GTP-labeled substrate RNA in 0.1 mM EDTA [pAT1 (P; 51 nt), Taq I pAT1 (T; 31 nt), Hinf I pAT1 (H; 24 nt), or 17-nt RNA] was mixed at room temperature with 0.1 mM EDTA (lanes 1 to 4) or unlabeled EGS RNA in 0.1 mM EDTA [29-nt EGS RNA (lanes 5 to 7), 20-nt EGS RNA (lanes 8 to 10), or 17-nt RNA (lanes 11 and 12)], and each mixture was incubated at 37°C in reaction buffer with (lanes 2 to 11) or without (lanes 1 and 12) unlabeled enzyme (*24*). Concentrations of substrates, EGS RNAs, M1 RNA, and C5 protein were 50, 60, 5, and 100 nM, respectively. (A) Reactions with M1 RNA were incubated for 100 min in 50 mM tris-HCl, pH 7.5, 100 mM $MgCl_2$, 100 mM NH_4Cl, 4% polyethylene glycol 6000–7500, and 0.06 mM EDTA. (B) Reactions with RNase P were incubated for 20 min in 50 mM tris-HCl, pH 7.5, 10 mM $MgCl_2$, 100 mM NH_4Cl, 0.06 mM EDTA, 0.2 mM sodium acetate, 1.2 mM NaCl, and 28 mM urea. Reactions were stopped by addition of formamide and excess EDTA, subjected to electrophoresis on 19% polyacrylamide gels that contained 7 M urea, and analyzed by autoradiography. The positions of the bromophenol blue marker dye (BB) and the 15-nt 5′ cleavage fragment of P are indicated. The cleavage fragment of T or H that comigrates with the 15-nt RNA is a 5′ cleavage fragment because it is the only radiolabeled product of cleavage by M1 RNA or RNase P of [γ-^{32}P]GTP-labeled T or H in the presence of 20- or 29-nt EGS RNA. The expected 3′ cleavage fragments of P, T, and H are 36, 16, and 9 nucleotides long, respectively (heterogeneity in uncleaved RNAs and 3′ cleavage fragments is due to heterogeneous termination of transcription by SP6 RNA polymerase). The 5′ and 3′ cleavage fragments of the 17-nt RNA are 6 and 11 nt long, respectively.

ished cleavage activity, demonstrating the importance of additional 2′-OH groups. The properties of 17-nt:dT, which is small enough to be synthesized chemically (*17*), may render it useful for the isolation of stable enzyme-substrate complexes.

Catalytic RNAs have been engineered to target unrelated sequences of RNA for specific cleavage in vitro (*18*) and, possibly, in vertebrate cells (*19*). On the basis of our work and given the wide variation in sequences of substrates for RNase P from *E. coli*, we propose that any RNA can be targeted for cleavage by RNase P from *E. coli* provided that an appropriately designed EGS RNA is included in the reaction (Fig. 1F). Evidence that the extra sequences shown at the bottom of the structure in Fig. 1F can be tolerated by RNase P is provided by an analysis of the structure of the precursor 4.5*S* RNA from *E. coli*, the only known, natural, non-tRNA substrate for RNase P (*20*). This RNA is proposed to contain a pAT1-like hairpin with a stem that has, in addition to several bulged loops, 44 base pairs (*20*). Although further work is necessary to evaluate the generality of the model in Fig. 1F, the activity of endogenous RNase P in any cell, such as the RNase P of human cells (*21*), could be directed to destroy specific messenger, viral, or other RNAs by the use of an appropriate EGS RNA. Such an application is analogous to the oligodeoxyribonucleotide-directed cleavage of RNAs in vivo by RNase H (*22*), but it has the advantage that EGS RNAs, unlike oligodeoxyribonucleotides, could be synthesized in vivo either separated from, or attached to, any transcript containing the RNA subunit of RNase P.

Small RNAs recently detected in the mitochondrion of *Leishmania tarentolae* have been proposed to form base pairs with precursor messenger RNAs to target them for cleavage by a postulated RNase P–like activity (*23*). This mechanism, which has been proposed to be involved in RNA editing (*23*), is remarkably similar to that of the reaction of RNase P of *E. coli* with Taq I pAT1–20-nt EGS RNA (Fig. 1D). Thus the targeting of RNAs by EGS RNAs for cleavage by RNase P may be a natural process in many organisms.

REFERENCES AND NOTES

1. F. Michel, A. Jacquier, B. Dujon, *Biochimie* **64**, 867 (1982); R. W. Davies, R. B. Waring, J. A. Ray, T. A. Brown, C. Scazzocchio, *Nature* **300**, 719 (1982); F. Michel, M. Hanna, R. Green, D. P. Bartel, J. W. Szostak, *ibid.* **342**, 391 (1989); A. Jacquier and F. Michel, *Cell* **50**, 17 (1987); A. C. Forster, C. Davies, C. C. Sheldon, A. C. Jeffries, R. H. Symons, *Nature* **334**, 265 (1988); J. Haseloff and W. L. Gerlach, *Gene* **82**, 43 (1989).
2. C. Guerrier-Takada, K. Gardiner, T. Marsh, N. Pace, S. Altman, *Cell* **35**, 849 (1983).
3. S. Altman, *Adv. Enzymol.* **62**, 1 (1989).
4. M. J. Fournier and H. Ozeki, *Microbiol. Rev.* **49**, 379 (1985).
5. W. H. McClain, C. Guerrier-Takada, S. Altman, *Science* **238**, 527 (1987).
6. The cleavage site was determined by labeling with [5′-^{32}P]pCp the 3′ end of the smaller cleavage fragment produced by cleavage of unlabeled 17-nt RNA by RNase P, digestion of the RNA to mononucleotides with RNase T2, and chromatography (*7*). The only radioactive nucleotide detected was uridine 3′-monophosphate.
7. A. C. Forster and R. H. Symons, *Cell* **49**, 211 (1987).
8. O. Orellana, L. Cooley, D. Soll, *Mol. Cell. Biol.* **6**, 525 (1986); C. Guerrier-Takada, A. van Belkum, C. W. A. Pleij, S. Altman, *Cell* **53**, 267 (1988).
9. C. Guerrier-Takada, W. H. McClain, S. Altman, *Cell* **38**, 219 (1984).
10. J.-Y. Lee and D. R. Engelke, *Mol. Cell. Biol.* **9**, 2536 (1989).
11. J.-Y. Lee and D. R. Engelke, personal communication.
12. J. R. Wyatt and G. T. Walker, *Nucleic Acids Res.* **17**, 7833 (1989).
13. The sole radiolabeled fragment after cleavage by RNase P of [α-^{32}P]dTTP-labeled 17-nt:dT has a slightly faster mobility during electrophoresis than that of [α-^{32}P]UTP-labeled 17-nt RNA. This result ruled out (i) incorporation of potentially contaminating [α-^{32}P]UTP instead of [α-^{32}P]dTTP (the mobility of the radiolabeled fragment would have been the same), (ii) incorporation of potentially contaminating unlabeled UTP together with α-^{32}P–labeled ATP or α-^{32}P–labeled CTP or α-^{32}P–labeled GTP (there would have been two radiolabeled fragments), and (iii) cleavage at a different site (the mobility of the radiolabeled fragment would have been slower, not faster). Reaction velocities were determined from the linear portion of plots of percent cleavage versus time. Greater than 20% cleavage of 17-nt:dT was obtained.
14. D. Herschlag and T. R. Cech, *Nature* **344**, 405 (1990); D. L. Robertson and G. F. Joyce, *ibid.*, p. 467.
15. T. L. Marsh and N. R. Pace, *Science* **229**, 79 (1985); C. Guerrier-Takada, K. Haydock, L. Allen, S. Altman, *Biochemistry* **25**, 1509 (1986).
16. W. Saenger, *Principles of Nucleic Acid Structure* (Springer-Verlag; New York, 1984).
17. N. Usman, K. K. Ogilvie, M.-Y. Jiang, R. J. Cedergren, *J. Am. Chem. Soc.* **109**, 7845 (1987).
18. A. J. Zaug, M. D. Been, T. R. Cech, *Nature* **324**, 429 (1986); J. Haseloff and W. L. Gerlach, *ibid.* **334**, 585 (1988); A. Hampel, R. Tritz, M. Hicks, P. Cruz, *Nucleic Acids Res.* **18**, 299 (1990).
19. M. Cotten and M. L. Birnstiel, *EMBO J.* **8**, 3861 (1989); F. H. Cameron and P. A. Jennings, *Proc. Natl. Acad. Sci. U.S.A.* **86**, 9139 (1989); N. Sarver *et al.*, *Science* **247**, 1222 (1990).
20. A. L. M. Bothwell, R. L. Garber, S. Altman, *J. Biol. Chem.* **251**, 7709 (1976); L. M. Hsu, J. Zagorski, M. J. Fournier, *J. Mol. Biol.* **178**, 509 (1984).
21. M. Bartkiewicz, H. Gold, S. Altman, *Genes Dev.* **3**, 488 (1989).
22. J. Walder, *ibid.* **2**, 502 (1988).
23. B. Blum, N. Bakalara, L. Simpson, *Cell* **60**, 189 (1990).
24. Truncated pAT1 RNAs, synthesized by SP6 RNA polymerase from the pGEM2-AT1 plasmid tem-

plate [(5); the digested templates with 3′-terminal single-stranded regions were incubated with the Klenow fragment of DNA polymerase I of *E. coli* before transcription], and the 17-nt RNA and EGS RNAs, synthesized by T7 RNA polymerase from oligodeoxyribonucleotide templates [J. F. Milligan, D. R. Groebe, G. W. Witherell, O. C. Uhlenbeck, *Nucleic Acids Res.* **15**, 8783 (1987)], were purified as described elsewhere (7). Wild-type M1 RNA and C5 protein were prepared as described elsewhere [A. Vioque, J. Arnez, S. Altman, *J. Mol. Biol.* **202**, 835 (1988)].

25. We thank D. Wesolowski for expert technical assistance, A. Vioque for C5 proteins, D. R. Engelke for access to unpublished data, and A. R. Benson, C. Guerrier-Takada, P. B. Moore, and M. Snyder for comments on the manuscript. A.C.F. is supported as The Merck Fellow of The Jane Coffin Childs Memorial Fund for Medical Research and was previously a fellow of The Anna Fuller Fund. Supported by grants NIH GM19422 and NSF DMB 8722644 to S.A.

30 March 1990; accepted 5 June 1990

An Essential Signaling Role for the m_3G Cap in the Transport of U1 snRNP to the Nucleus

UTZ FISCHER AND REINHARD LÜHRMANN

The major small nuclear ribonucleoprotein particles (snRNPs) U1, U2, U4 + U6, and U5 have to be transported from the cytoplasm, where they are synthesized, to the nucleus, where they splice pre–messenger RNAs. Since the free core snRNP proteins in the cytoplasm do not enter the nucleus on their own, the nuclear location signal must either reside on the snRNA or be created as a result of snRNA-protein interaction. Here the involvement by the 5′-terminal cap of snRNA molecules in the nucleo-cytoplasmic transport of UsnRNPs has been studied by microinjection of synthetic U1 RNA molecules into frog oocytes; the U1 RNA bore either the normal cap (m_3G) or a chemical derivative. Antibodies in the cytoplasm against the m_3G cap inhibited the nuclear uptake of U1 snRNP. U1 RNA that was uncapped or contained an unnatural ApppG cap did not enter the nucleus, even though it carried a normal complement of protein molecules. When the ribose ring of the m_3G cap was oxidized with periodate, nuclear transport of U1 snRNPs was severely inhibited. Finally, microinjection of m_3G cap alone (but not m^7G cap) into oocytes severely inhibited the transport of U1 snRNPs to the nucleus. These data suggest that one step in the nuclear uptake of U1 snRNPs involves the m_3G cap structure.

THE TRANSPORT OF MACROMOLECULES between the cytoplasm and the nucleus appears to occur through pores in the nuclear membrane (*1–3*). Although some small proteins may diffuse passively into the nucleus, many proteins contain one or more "nuclear location signals" that direct them to the nucleus (*4, 5*), possibly by an active transport mechanism (*6, 7*). It is not yet known how larger particles such as U snRNPs are transported to the nucleus (*8*).

The proteins of the major spliceosomal snRNPs U1, U2, U4 + U6, and U5 can be divided into two classes: the proteins common to all these particles [also called Sm proteins (*9*)] and proteins that are associated specifically with U1, U2, or U5 (*10*). In *Xenopus* oocytes (*11*) and in somatic cells (*12*) the common proteins are synthesized in excess over U snRNAs and remain in the cytoplasm. Only after association of these proteins with newly transcribed U snRNA precursor molecules are the cytoplasmic snRNP proteins transported as an RNP particle to the nucleus. Microinjection studies with mutant U2 RNA genes have shown that association of the common proteins with the U2 RNA is necessary for efficient nuclear transport (*13*), whereas the presence of U2-specific proteins on the particle is not required (*14*). Since free Sm proteins do not enter the nucleus, the nuclear location signal must either reside on the snRNA or be created as a result of snRNA-protein interaction, for example, by a conformational change in the Sm proteins that exposes a nuclear location signal (*15*).

We decided to test the first possibility by seeking a determinant of nuclear transport lying on the snRNA. All U snRNA species except U6 RNA have an m_3G cap at their 5′ ends (*16*), with the sequence m_3GpppG (m_3G is 2,2,7-trimethyl guanosine); U6 RNA carries a γ-monomethyl phosphate at its 5′ end (*17*). The m_3G cap is formed in the cytoplasm by dimethylation of an m^7G cap (m^7GpppG, where m^7G is 7-methyl guanosine). It is in keeping with a role for the m_3G cap as nuclear location signal that the dimethylation does not occur until after the Sm snRNP proteins have assembled onto the pre-snRNA (*18*), that is, when the newly formed snRNP particle is ready to move to the nucleus.

We tested whether m_3G had a signaling role with a chemically synthesized m_3GpppG cap (*19*). We attached this cap at the 5′ end of U1 RNA by using it as primer for RNA polymerase SP6-directed synthesis of U1 snRNA from a suitably constructed plasmid. In this way, capped U1 snRNA and related derivatives were prepared in vitro.

We then tested whether antibodies to the m_3G cap structure (anti-m_3G) were able to inhibit the nuclear transport of U1 snRNPs. Increasing amounts of a monoclonal anti-m_3G (*20*) were coinjected with m_3G-capped human U1 snRNA (*21*) into the cytoplasm of *Xenopus laevis* oocytes. The injected radioactive U1 snRNA was transported efficiently to the nucleus, whereas the anti-m_3G severely inhibited this transport (at the highest antibody concentration, the rate of nuclear uptake was reduced by about 95%) (Fig. 1A). Coinjection of a monoclonal antibody (MAb) to a non-snRNP protein had no effect (Fig. 1B). The binding of U1 RNA to the Sm snRNP proteins was not impaired by the presence of anti-m_3G, as indicated by the precipitability of U1 RNA with a monoclonal anti-Sm (Fig. 1C). Although the bulky anti-m_3G molecule may sterically hinder the passage of U1 snRNP through the nuclear pores, such hindrance is unlikely, as immunoglobulin G (IgG) molecules bound to large karyophilic proteins are known to be cotransported to the nucleus (*22, 23*).

When we injected uncapped U1 RNA (that is, U1 RNA with pppG at its 5′ terminus) into the cytoplasm of oocytes, the injected RNA molecules remained stable for more than 30 hours, but no nuclear transport was observed (Fig. 2A, exp. 2) despite the fact that the U1 RNA was assembled efficiently into U1 RNP particles containing all their Sm proteins (Fig. 2C, exp. 2).

Anti-m_3G did not react with the cytoplasmic U1 RNAs or RNPs (Fig. 2B, exp. 2), showing that no cap structures had been added to the injected U1 RNA molecules in the cytoplasm. It was possible that uncapped U1 snRNPs might have entered the nucleus and eluded detection because of rapid degradation of "naked" RNA inside the nucleus. However, we could not detect any RNA molecules or radioactivity in the nucleus at 1, 2, 3, 6, or 12 hours after the oocytes were injected and the U1 RNA concentration in the cytoplasm remained roughly constant during a 30-hour period (*24*).

We tested 5′-terminal caps other than m_3G, but none of these led to the transport of U1 RNPs to the nucleus. U1 RNA

Institut für Molekularbiologie und Tumorforschung, der Philipps-Universität Marburg, Emil-Mannkopff-Strasse 2, D-3550 Marburg, Federal Republic of Germany.